Supplementary information

Supplementary Equation

The Susceptible-Infectious-Recovered Model

The model simulates four key processes governing tau dynamics: **spread, synthesis, clearance, and misfolding**. Equations (1)–(4) formally describe how region-specific vulnerability input parameters independently modulate each process, determining the resulting concentrations of normal (N_i) and misfolded (M_i) tau in each region i over discrete time steps.

At each simulation step, tau dynamics are updated sequentially through spreading, synthesis, clearance, and misfolding. Protein flux between axonal compartments and regional cell bodies is explicitly modeled during the spreading step, whereas synthesis and clearance operate locally within each region. All state variables at time t depend on the protein concentrations from the previous time step ($t-1$).

During the **spread** process, the normal or misfolded protein concentration in region i (P_i) is determined by the proteins retained from the previous time step ($P_{i,t-1}$) and the flux of proteins exchanged between the axon/terminal (edge) and the soma (region). Specifically, $P_{i,incoming}$ represents the number of tau proteins transported from the connected axons (presynaptic regions) to the soma of region i (postsynaptic target), while $P_{i,outgoing}$ denotes the number of tau proteins conveyed from the soma toward its axons/terminals within region i, , reflecting anterograde axonal transport. The extended input parameter $\mathbf{spread\_rate}_i$ allows regional modulation of tau spread, controlling the amount of tau transferred from presynaptic regions to the soma of region i, scaled by the time increment Δt.

$$P_i = P_{i,t-1} + P_{i,\text{incoming}} \times \mathbf{spread\_rate}_i \times \Delta t - P_{i,\text{outgoing}} \tag{1}$$

The **synthesis** process follows spreading. The number of newly produced normal proteins in region i ($N_{i,synthesized}$) is determined by the global synthesis rate across the brain ($\text{synthesis\_rate}_{global}$) and the input region-specific synthesis rate ($\mathbf{synthesis\_rate}_i$). The number of proteins synthesized within a time interval Δt is constant for each region and independent of the existing protein concentration.

$$N_{i,\text{synthesized}} = \left(\text{synthesis\_rate}_{global} \times \mathbf{synthesis\_rate}_i\right) \times \Delta t \tag{2}$$

The **clearance** process occurs concurrently with synthesis over a short time interval Δt. The number of normal or misfolded proteins cleared from region i ($P_{i,cleared}$) depends on the current protein number after spreading (P_i) and the input regional clearance rate ($\mathbf{clearance\_rate}_i$).

$$P_{i,\text{cleared}} = P_i \times \left(1 - e^{-\mathbf{clearance\_rate}_i \times \Delta t}\right) \tag{3}$$

During the **misfolding** process, the number of newly misfolded proteins in region i ($M_{i,misfolded}$) is determined by the remaining pool of normal proteins after the clearance process ($N_i \times e^{-\text{clearance\_rate}_i}$), the current level of misfolded protein after the spreading process (M_i), the global misfolding probability ($\text{misfold\_rate}_{global}$), and the input regional misfolding rate ($\mathbf{misfold\_rate}_i$). The extended parameter $\mathbf{misfold\_rate}_i$ provides regional control over the misfolding propensity of tau.

$$M_{i,\text{misfolded}} = N_i \times e^{-\text{clearance\_rate}_i} \times \text{misProb}_{\text{global}} \times \mathbf{misfold\_rate}_i \quad (4)$$

where $\text{misProb}_{\text{global}} = 1 - e^{-M_i \times \text{misfold\_rate}_{global} \times \Delta t}$

During each simulation step, the combined effects of these processes determine the updated levels of normal (N_i) and misfolded (M_i) proteins in region i at time t. The resulting concentrations are expressed as:

$$N_i = P_i - P_{i,cleared} - M_{i,misfolded} + N_{i,synthesized} \quad (5)$$

$$M_i = P_i - P_{i,cleared} + M_{i,misfolded} \quad (6)$$

Supplementary Notes

Supplementary Note 1. Participant inclusion and diagnostic criteria

The Swedish BioFINDER-2 study enrolls participants across multiple clinical stages of cognitive impairment. The present study included participants from Cohorts A-D; individuals with non–Alzheimer's disease neurodegenerative disorders (Cohort E) were not included.

Cohorts A and B comprised neurologically and cognitively unimpaired individuals aged 40–65 years (Cohort A) or 66–100 years (Cohort B). Inclusion criteria were: (i) absence of cognitive symptoms as assessed by a physician with expertise in cognitive disorders; (ii) Mini-Mental State Examination (MMSE) score of 27–30 (Cohort A) or 26–30 (Cohort B) at screening; (iii) no fulfillment of criteria for mild cognitive impairment (MCI) or dementia according to DSM-5; and (iv) fluency in Swedish. Recruitment of these cohorts was designed to achieve approximately equal proportions of APOE ε4 carriers.

Cohort C included participants aged 40–100 years referred to memory clinics due to cognitive complaints. Inclusion criteria were: (i) MMSE score of 24–30; (ii) absence of dementia according to DSM-5; and (iii) fluency in Swedish. Participants were classified as having MCI if they performed worse than −1.5 standard deviations relative to age- and education-adjusted norms in at least one cognitive domain. Cognitive assessment covered attention/executive function (Trail Making Test A and B, Symbol Digit Modalities Test, AQT), memory (immediate and delayed recall from the Alzheimer's Disease Assessment Scale), language (verbal fluency and short Boston Naming Test), and visuospatial function (Visual Object and Space Perception battery). Participants who did not meet MCI criteria were classified as having subjective cognitive decline (SCD). In accordance with the NIA–AA research framework, individuals with SCD were grouped together with cognitively unimpaired participants in analyses where appropriate.

Cohort D comprised participants aged 40–100 years referred to memory clinics who fulfilled DSM-5 criteria for dementia (major neurocognitive disorder) due to Alzheimer's disease. Inclusion criteria included an MMSE score ≥12 and fluency in Swedish.

Across all cohorts, exclusion criteria were: (i) significant unstable systemic illness interfering with study participation; (ii) current significant alcohol or substance misuse; and (iii) refusal to undergo lumbar puncture, MRI, or PET imaging.

Supplementary Note 2. Details of PET acquisition and preprocessing

Tau PET imaging was performed using [^{18}F]RO948 on a digital scanner (Discovery MI; GE Healthcare). PET data were acquired in 70 to 90 minutes post-injection.

Low-dose computed tomography scans were acquired immediately prior to PET imaging for attenuation correction. Image reconstruction was performed using VPFX-S (ordered subset expectation maximization combined with corrections for time-of-flight and point spread function) with 6 iterations, 17 subsets, and applied 3-mm Gaussian smoothing, a standard Z filter, and a 25.6-cm field of view (256 × 256 matrix). List-mode data were binned into four consecutive 5-minute frames.

PET frames were motion corrected using rigid-body realignment implemented in AFNI (*3dvolreg*), summed within participant, and rigidly coregistered to the corresponding native-space T1-weighted MRI. Subsequent intensity normalization using an inferior cerebellar gray matter reference region yielded standardized uptake value ratio (SUVR) images, which were used for regional quantification as described in the main Methods.

Supplementary Note 3. Hyperparameter tuning

For all SIR model simulations, hyperparameters were systematically tuned to optimize correspondence between simulated and observed tau patterns. The parameter search space

included the probability of tau remaining within the neuronal cell body (**stay probability**; values: 0.01, 0.05, 0.1, 0.3, 0.5, 0.7, 0.9), the global tau misfolding rate (**transform rate**; values: 0.1, 0.5, 0.9, 1.0, 1.5, 1.9, 2.0, 2.5, 2.9, 3.0), and tau spreading velocity along anatomical connections (**velocity**; values: 0.1, 0.3, 0.5, 0.7, 0.9, 1.0). For each combination of parameters, model performance was evaluated based on its ability to reconstruct group-averaged regional tau presence (TPP) or tau load (SUVR). The parameter set yielding the best fit was then selected for subsequent analyses.

Supplementary Note 4. Epidemic spreading model

The spread of tau pathology across connected brain regions was simulated using the Epidemic Spreading Model (ESM), a previously described diffusion-based framework applied to misfolded protein propagation in neurodegenerative disease. The ESM models the diffusion of a pathological signal from a predefined epicenter through a weighted brain connectome over time. Model dynamics are governed by subject-specific parameters describing global tau production rate, clearance rate, and estimated age of onset, which modulate the overall extent of spread without determining regional patterning.

The ESM was fit within-subject using regional tau presence (TPP) or tau load (SUVR) as input, represented as region-by-subject matrices. For the primary analyses, the left and right entorhinal cortex were selected as model epicenters based on neuropathological evidence of early tau accumulation. Model predictions were compared to observed regional tau patterns, and performance was quantified based on the correspondence between predicted and observed values. Consistent with prior work, the free parameters primarily controlled global tau burden, allowing the model to accommodate individuals across the Alzheimer's disease spectrum.

Supplementary Note 5. *Franzmeier et al., 2020* statistical approach

To further assess the relationship between anatomical connectivity and tau propagation, we performed connectivity-based statistical analyses following previously described approaches. Cross-sectionally estimated tau spreading matrices were constructed by concatenating regional tau presence or tau load across Aβ-positive participants. Rows (subjects) and columns (regions) were rank-ordered by their respective means, yielding tau positivity sequences.

Epicenters were defined as the 10% of regions exhibiting the earliest tau involvement. Mean connectivity-based distance from these epicenters was calculated using the structural connectome employed in the SIR and ESM analyses. Associations between tau spreading sequences and connectivity-based distances were assessed using linear regression.

Supplementary Figures

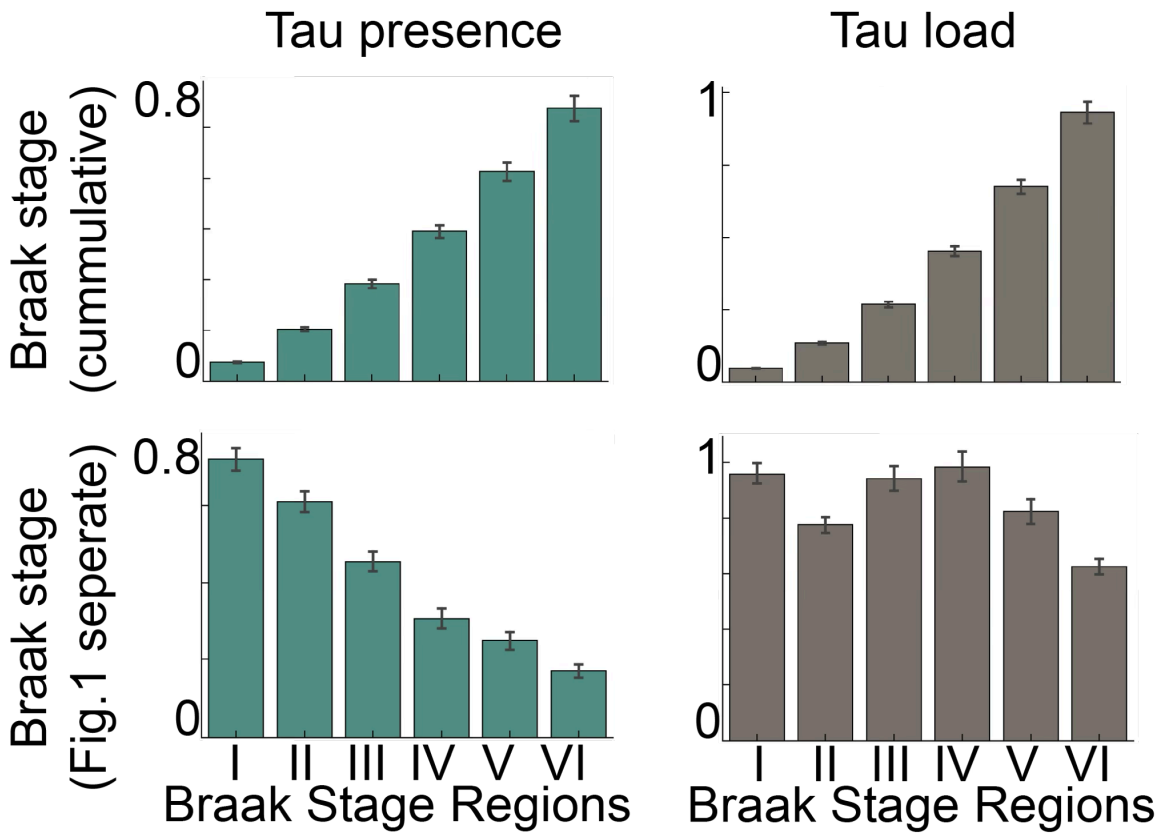

Fig. S1. Accumulative versus separate Braak stage definitions for tau presence and load. Mean ± SEM values of tau presence (left) and tau load (right) across Braak stage regions. Top: values calculated accumulatively, including regions from earlier stages. Bottom: values calculated separately, including only regions of the corresponding stage (approach used in the main manuscript, Fig. 1). The latter approach is a better approximation to Braak staging, where braak stage regions are addressed independently.

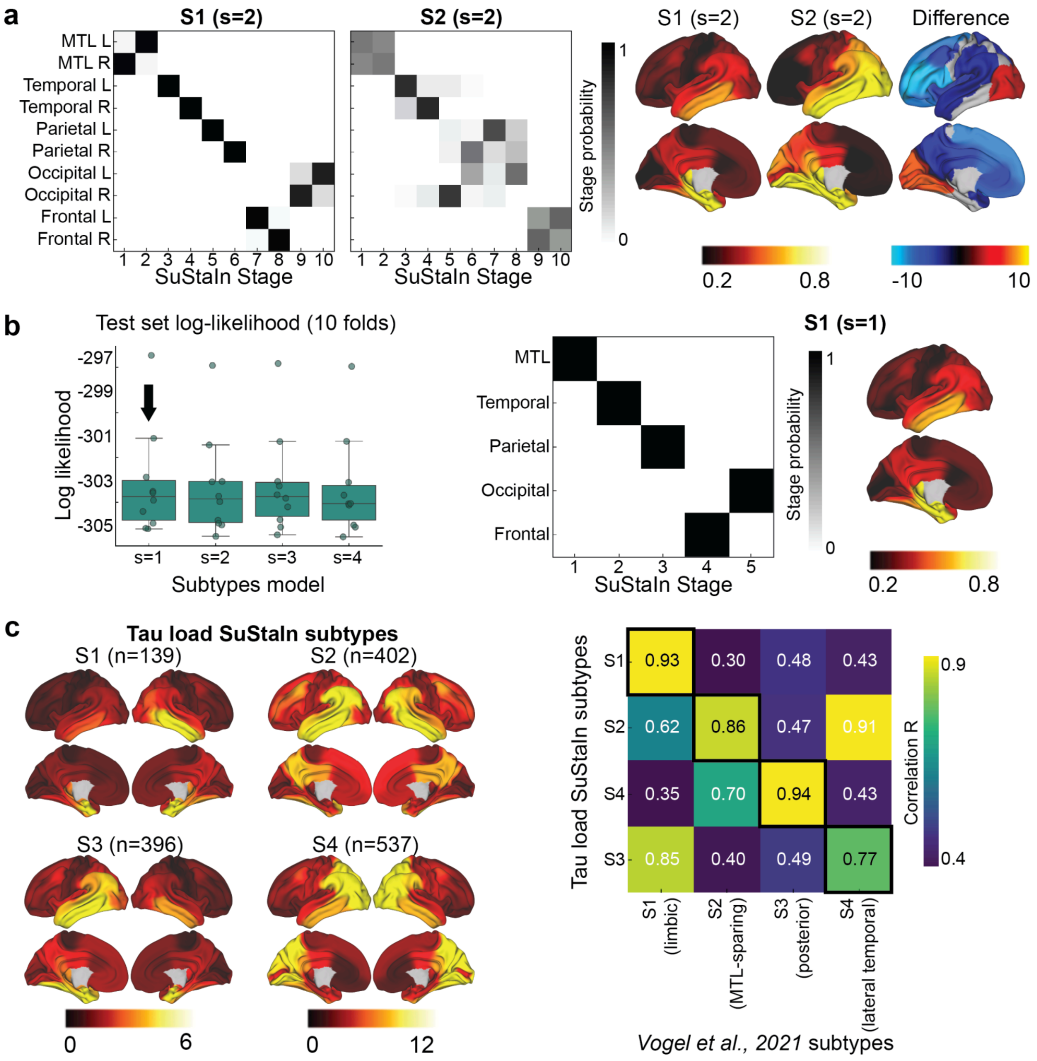

Fig. S2. Tau presence is consistent across individuals, tau load is heterogeneous, Related to main text Fig. 1 and Fig. 5.

a) Left: Positional variance for two identified tau presence subtypes using 10 brain regions. Each box represents the confidence that a brain region has reached a certain pathology level at a given SuStaIn (disease progression) stage, with darker colors indicating higher certainty. Right: Tau presence cortical surface projections for the two subtypes and a difference map. **b)** Results using five brain regions. Left: For each subtype model (k=1–4), the distribution of average negative log-likelihood across cross-validation folds of left-out individuals is shown (higher log-likelihood indicates better model fit). Middle: Positional variance for two tau presence subtypes. Right: Tau presence cortical surface projections of the identified tau presence subtype. **c)** Right: Brain map for the identified four tau load subtypes. Left: Confusion matrix comparing subtypes identified in the current study (SuStaIn subtypes; y-axis) with those from *Vogel et al., 2021* (x-axis). Values represent spatial correlations between average regional tau for each subtype. Diagonal values indicate subtype similarity across both parameter sets. L: left; R: right; SuStaIn: Subtype and Stage Inference model.

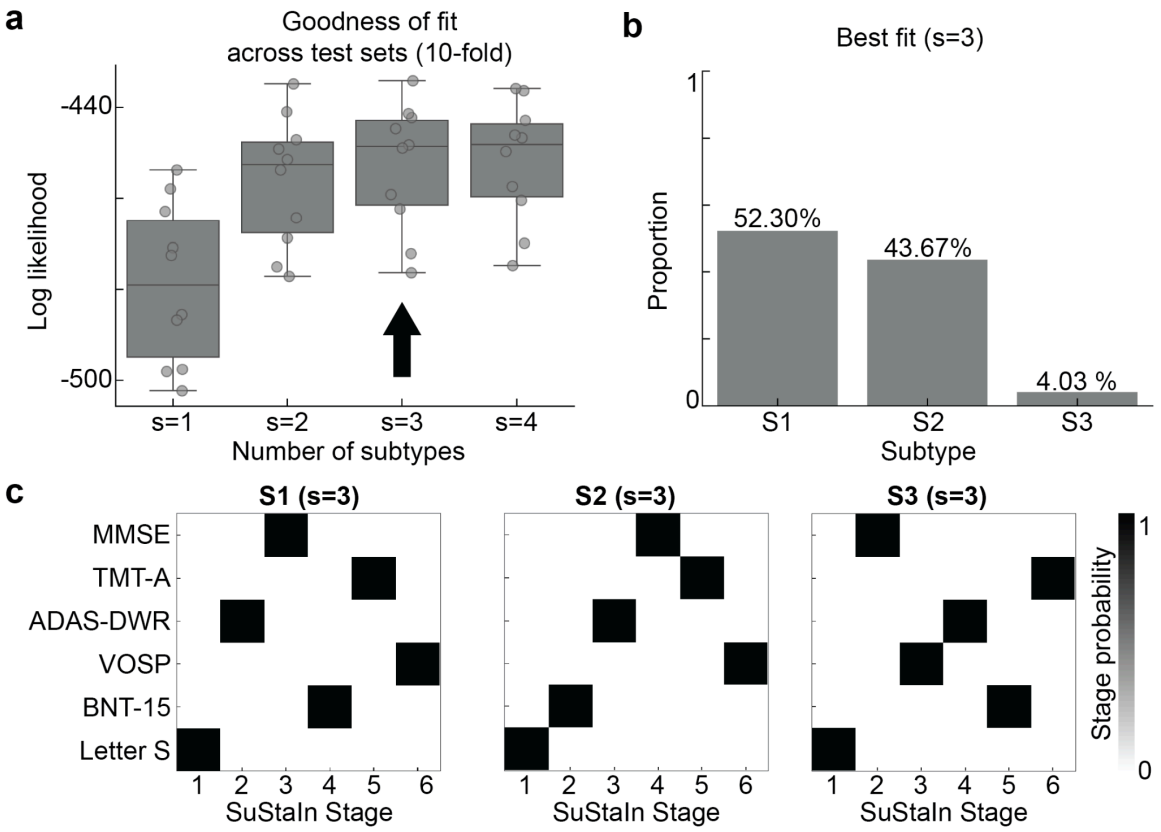

Fig. S3. SuStaIn-derived three spatiotemporal patterns for cognitive positive-probabilty. Related to main text Fig. 1.

To prove that the binarizing data does not automatically lead to a lack of subtypes, binarized cognitive data and ran SuStaIn on this data. Six cognitive measurements were first transformed into cognitive positive-probability (presence of cognitive domain impairment) using two-component Gaussian Mixture model, following the same exact procedure performed to calculate tau presence. A SuStaIn model was then applied on binarized cognitive impairment of six measures. **a)** For each subtype model (s=1-4), distributions of average negative log-likelihood across 10 cross-validation folds of left-out individuals are shown, higher values indicate better fit. The best-fit model is marked by the black arrow. **b)** Bar plots show the proportion of participants assigned to each subtype. **c)** Positional variance for three cognitive domain impairment sequence subtypes. SuStaIn: Subtype and Stage Inference; MMSE: mini-mental state examination; TMT-A: trail making test A; ADAS-DWR: Alzheimer's Disease Assessment Scale, delayed word recall; VOSP: Visual Object and Space Perception Battery; BNT-15: Boston Naming Test - short form; Letter S: letter S fluency test.

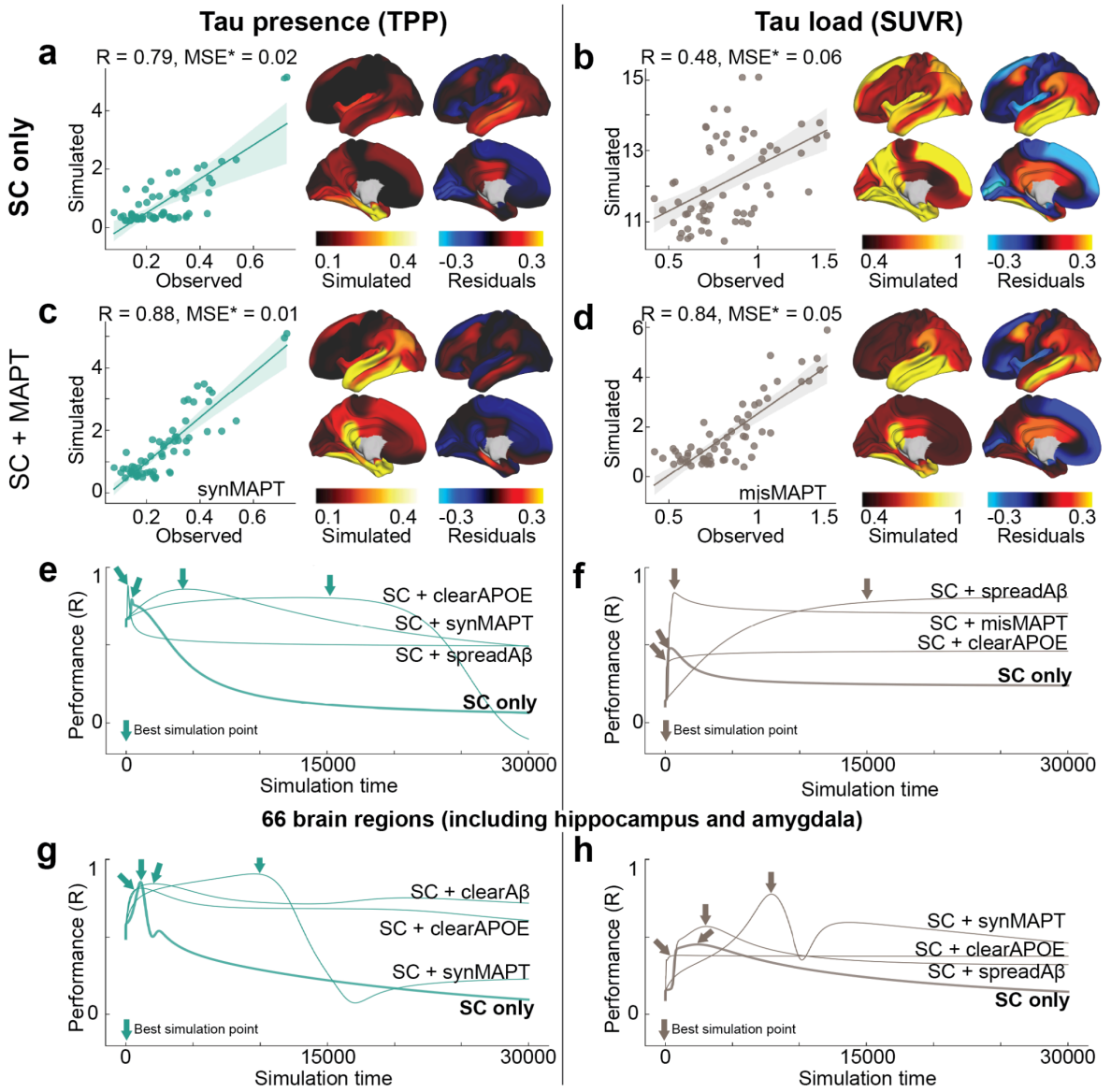

Fig. S4. Replication of main text Fig. 2 using a different structural connectome.
Results of the SIR model simulating tau diffusion through a structural connectome (derived from healthy young individuals from HCP) using an entorhinal cortex epicenter. Note that hippocampus and amygdala are not included in this connectome.
a, b) Model performance for tau presence (TPP) a), and tau load (SUVR) b). Scatter plots compare SIR model predictions to observed tau TPP/SUVR, while cortical surface projections show simulated tau presence and model residuals. Residuals represent the difference between observed tau values and simulated tau values, with the simulated values normalized to the range of observed values. **c-h)** To assess the influence of regional vulnerability on tau propagation, three regional properties were incorporated into the model: *MAPT* expression, *APOE* expression, and Aβ deposition. c, d) The best-fitting regional property influencing tau presence (SC plus *MAPT* expression affecting regional synthesis) is shown in c), and for tau load in d). **e, f)** Model performance (SC only vs. SC with three regional properties) over simulated time for TPP and SUVR, respectively. **g, h)** Model performance (SC only vs. SC with three regional properties, simulated with 66 brain regions used in Fig. 2) over simulated time for TPP and SUVR, respectively. MSE* was calculated using normalized simulated values (scaled to the range of observed tau values) to ensure a fair comparison, as the model lacks constraints on simulated values, which can increase without limit. SUVR: standardized uptake value ratio; TPP: tau positive-probability; SC: structural connectivity; R: Pearson correlation coefficient; MSE: mean squared error; *MAPT*: microtubule associated protein tau; *APOE*: Apolipoprotein E; syn: synthesis; clear: clearance; mis: misfold.

Supplementary Tables

Table S1. Sample characteristics.

	BioFINDER2
Participants (N)	646
Diagnosis (%Normal/MCI/AD)	33.90/32.82/33.28
Age (yrs)	73.27 (7.73) [44.26 - 93.26]
Gender (F/M)	325/321
Education (yrs)	12.61 (4.12) [3.00 - 33.00]
APOE4 (carrier/non-carrier)	408/178
CSF Aβ42/40	0.05 (0.01) [0.02 - 0.08]
CSF p-tau217 (pgml)	403.24 (327.35) [19.10 - 2016.15]

Mean (standard deviation) [minimum, maximum] values are reported for continuous variables, and participant counts are provided for categorical variables (Participants, Diagnosis, Gender, APOE4).

% = percentage; MCI = Mild Cognitive Impairment; AD = Alzheimer's Disease; yrs = years old; F = female; M = male; CSF = cerebral spinal fluid; Aβ + = β amyloid positive

Table S2. Model performance for simulating tau progression along anatomical connections (66 regions, including hippocampas and amygdala), influenced by regional classical AD-related elements. Related to Fig. 2.

Models	Tau presence (TPP)				Tau load (SUVR)			
	R	MSE*	Hyperparams	Time	R	MSE*	Hyperparams	Time
SC only	**0.8560**	**0.0195**	(0.7, 1.9, 0.1)	1101	**0.4534**	**0.0723**	(0.9, 1.5, 0.1)	2412
+spreadMAPT	0.6843	0.0310	(0.9, 1.5, 0.1)	742	0.4803	**0.0604**	(0.9, 1.9, 0.1)	4372
+syn*MAPT*	**0.9083**	**0.0102**	(0.05, 2.5, 0.1)	9540	**0.7777**	0.0615	(0.01, 3, 0.1)	7898
+mis*MAPT*	0.7495	0.0252	(0.1, 3, 0.5)	2044	0.7017	0.0659	(0.3, 2.9, 0.5)	1836
+clear*MAPT*	0.8404	0.0233	(0.1, 0.5, 0.9)	1970	0.2848	0.1743	(0.9, 0.1, 0.1)	248
+spreadAβ	0.6833	**0.0268**	(0.9, 1.5, 0.1)	765	**0.5694**	**0.0546**	(0.9, 1.5, 0.1)	3048
+synAβ	0.7347	0.0358	(0.01, 2, 0.1)	11757	0.4280	0.1506	(0.9, 3, 1)	69
+clearAβ	0.7235	0.0312	(0.01, 3, 0.1)	9694	0.4590	0.1498	(0.5, 2.9, 0.1)	2943
+misAβ	**0.8447**	0.0240	(0.05, 0.5, 0.7)	2101	0.2894	0.1605	(0.01, 0.5, 0.1)	16812
+spread*APOE*	0.7475	0.0262	(0.9, 0.1, 1)	29999	0.3384	**0.0737**	(0.9, 1.5, 0.1)	1077
+syn*APOE*	0.7171	0.0282	(0.01, 1, 1)	4512	0.3296	0.0865	(0.01, 3, 0.7)	29999
+mis*APOE*	0.7140	0.0370	(0.01, 1.5, 0.1)	13202	0.2558	0.1713	(0.01, 1, 0.1)	16248
+clear*APOE*	**0.8161**	**0.0223**	(0.05, 0.5, 1)	1158	**0.3829**	0.1018	(0.9, 3, 1)	1112

Each regional canonical AD-related element was parameterized to influence tau simulation via spread, synthesis, misfolding, and clearance rates. All models underwent hyperparameter tuning, and the best-performing model was selected based on the highest simulation accuracy at the optimal time point (total time = 30,000) and hyperparameter set. The best-performing model for each AD-related element is highlighted in bold. Selected hyperparameters, including stay probability, transform rate, and velocity, are shown.

* MSE was calculated using normalized simulated tau values, scaled to match the range of observed tau.

TPP = tau-positive probability; SUVR = standardized uptake ratio; R = Pearson correlation coefficient; MSE = mean squared error; SC = structural connectivity; syn = synthesis; mis = misfold; clear = clearance; Aβ = β amyloid

Table S3. Model performance for simulating tau progression along anatomical connections (62 regions, excluding hippocampas and amygdala), influenced by regional classical AD-related elements. Related to Fig. S4.

Models	Tau presence (TPP)				Tau load (SUVR)			
	R	MSE*	Hyperparams	Time	R	MSE*	Hyperparams	Time
SC only	**0.7941**	**0.0178**	(0.9, 1.9, 0.1)	425	**0.4785**	**0.0633**	(0.9, 2.5, 1)	403
+spreadMAPT	0.8338	0.0093	(0.01, 0.9, 1)	10718	0.6911	**0.0492**	(0.9, 3, 0.1)	5076
+syn*MAPT*	**0.8818**	**0.0074**	(0.9, 3, 0.9)	141	0.8268	0.0513	(0.9, 3, 0.1)	857
+mis*MAPT*	0.8711	0.0093	(0.5, 1.5, 0.7)	3399	**0.8384**	0.0509	(0.9, 3, 0.1)	679
+clear*MAPT*	0.7352	0.0283	(0.01, 0.1, 0.1)	29999	0.2223	0.1731	(0.01, 0.1, 0.1)	29999
+spreadAβ	**0.8593**	**0.0097**	(0.01, 0.5, 1)	4490	**0.8084**	**0.0371**	(0.01, 0.1, 1)	29999
+synAβ	0.7185	0.0295	(0.01, 1.5, 0.7)	1182	0.4963	0.0894	(0.9, 3, 0.1)	177
+clearAβ	0.8075	0.0193	(0.01, 3, 0.1)	13652	0.2716	0.1539	(0.01, 0.1, 0.1)	29999
+misAβ	0.7659	0.0234	(0.01, 0.1, 0.1)	21076	0.4479	0.1449	(0.9, 3, 0.5)	118
+spread*APOE*	0.7493	0.0190	(0.9, 3, 0.1)	223	0.4107	**0.0648**	(0.9, 3, 1)	223
+syn*APOE*	0.7516	0.0183	(0.01, 0.9, 0.5)	14765	0.4142	0.1481	(0.01, 3, 1)	29811
+mis*APOE*	0.7490	0.0268	(0.01, 0.1, 0.1)	29999	0.2458	0.1612	(0.01, 0.9, 0.1)	29999
+clear*APOE*	**0.8067**	**0.0168**	(0.01, 1, 0.1)	12965	**0.4595**	0.0915	(0.5, 3, 1)	29999

Each regional canonical AD-related element was parameterized to influence tau simulation via spread, synthesis, misfolding, and clearance rates. All models underwent hyperparameter tuning, and the best-performing model was selected based on the highest simulation accuracy at the optimal time point (total time = 30,000) and hyperparameter set. The best-performing model for each AD-related element is highlighted in bold. Selected hyperparameters, including stay probability, transform rate, and velocity, are shown.

* MSE was calculated using normalized simulated tau values, scaled to match the range of observed tau.

TPP = tau-positive probability; SUVR = standardized uptake ratio; R = Pearson correlation coefficient; MSE = mean squared error; SC = structural connectivity; syn = synthesis; mis = misfold; clear = clearance; Aβ = β amyloid.

Table S4. Performance of models better than null for tau presence and load, Related to Fig. 3.

(Attached Supplementary_Table4_Presence-Load_mdoels_performance.xlsx)

The optimal time points (total time = 30,000) are provided, along with the selected hyperparameters: stay probability, transform rate, and velocity.
* MSE was calculated using normalized simulated tau values, scaled to match the range of observed tau.

$EV\left(y,\ \hat{y}\right) = 1 - \frac{variance\{y-\hat{y}\}}{varicance\{y\}}$

R = Pearson correlation coefficient; EV = explained variance; MSE = mean squared error; syn = synthesis; mis = misfold; clear = clearance; Aβ = β amyloid; SC = structural connectivity; FC = functional connectivity; GC = gene coexpression; NS = neurotransmission markerreceptor similarity; LS = laminar similarity; MC = metabolic covariance; EP = electrophysiological; TS = temporal similarity; CBF: cerebral blood flow; CBV: cerebral blood volume; thickness: cortical thickness; scaling: allometric scalling.

Table S5. Top 10 performing models for four tau subtypes. Related to Fig. 5.

Rank	Conn	Factor type	Factor	Rate	epicenter	R	MSE*	EV	Time	Hyperparam
S1 (limbic)										
1	NS	AD-related	*MAPT*	mis	entorhinal	0.862845	0.034825	0.744296	309	(0.7, 2.5, 1)
2	**SC**	**AD-related**	**Aβ**	**spread**	**entorhinal**	**0.857989**	**0.057556**	**0.681557**	**26603**	**(0.01, 0.1, 1)**
3	**SC**	**AD-related**	***MAPT***	**mis**	**entorhinal**	**0.829726**	**0.102957**	**0.667079**	**644**	**(0.7, 2, 1)**
4	FC	Metabolism	CBF	clear	entorhinal	0.829574	0.083759	0.670772	109	(0.3, 2.5, 0.5)
5	NS	Neurotransmission	D_2	syn	entorhinal	0.820716	0.077905	0.672382	249	(0.7, 0.9, 1)
6	MC	AD-related	*MAPT*	spread	entorhinal	0.811984	0.064914	0.616343	305	(0.01, 1.5, 1)
7	NS	Cortical expansion	scaling	spread	entorhinal	0.806169	0.075119	0.643618	176	(0.7, 1.5, 1)
8	GC	Neurotransmission	D_2	mis	entorhinal	0.804641	0.130564	0.616469	128	(0.5, 3, 0.5)
9	NS	Cortical expansion	scaling(PNC)	spread	entorhinal	0.804529	0.075598	0.623521	386	(0.9, 1, 1)
10	**SC**	**Metabolism**	**cbf**	**clear**	**entorhinal**	**0.803622**	**0.108175**	**0.612997**	**232**	**(0.01, 2, 1)**
S2 (MTL-sparing)										
1	FC	AD-related	*MAPT*	syn	precuneus	0.791723	0.109894	0.621974	246	(0.7, 2, 0.1)
2	FC	Neurotransmission	5-HT_4	spread	precuneus	0.748243	0.100595	0.502537	296	(0.01, 0.9, 1)
3	FC	AD-related	Aβ	mis	precuneus	0.745201	0.106030	0.530556	288	(0.5, 3, 0.3)
4	FC	Neurotransmission	MOR	spread	precuneus	0.723219	0.080160	0.401855	369	(0.9, 1.5, 0.5)
5	FC	Cortical expansion	evoexp	spread	precuneus	0.713213	0.105971	0.395552	470	(0.9, 1.5, 0.1)
6	**SC**	**AD-related**	***MAPT***	**mis**	**precuneus**	**0.679672**	**0.104747**	**0.436256**	**29999**	**(0.7, 1.5, 0.7)**
7	FC	Microstructure	thickness	spread	precuneus	0.679093	0.099393	0.329833	333	(0.9, 1.5, 1)
8	NS	AD-related	*MAPT*	syn	precuneus	0.675587	0.115101	0.440080	181	(0.7, 2.9, 0.1)
9	FC	Cortical expansion	scaling(HCP)	syn	precuneus	0.671264	0.126692	0.401385	310	(0.9, 1.5, 0.1)
10	FC	Neurotransmission	5-HT_{1A}	spread	entorhinal	0.664754	0.093338	0.347357	312	(0.9, 1.9, 1)
S3 (posterior)										
1	FC	Neurotransmission	VAChT	clear	precuneus	0.827086	0.077399	0.683300	58	(0.7, 3, 0.7)
2	FC	Neurotransmission	H_3	clear	precuneus	0.818289	0.082730	0.641840	188	(0.9, 1, 1)
3	**SC**	**Neurotransmission**	**VAChT**	**clear**	**entorhinal**	**0.806718**	**0.074583**	**0.630937**	**84**	**(0.7, 3, 1)**
4	LS	Neurotransmission	VAChT	clear	precuneus	0.799226	0.081894	0.624025	457	(0.9, 0.5, 0.1)
5	**SC**	**Neurotransmission**	**H_3**	**clear**	**entorhinal**	**0.785744**	**0.157704**	**0.617262**	**135**	**(0.7, 3, 1)**
6	FC	Neurotransmission	$\alpha_4\beta_2$	clear	precuneus	0.779143	0.076642	0.546371	583	(0.9, 0.5, 1)

7	MC	Neurotransmission	H3	clear	precuneus	0.777362	0.179316	0.598003	7036	(0.01,1.5,0.1)
8	EP	Neurotransmission	VAChT	clear	precuneus	0.775874	0.101134	0.567764	82	(0.9, 3, 0.1)
9	LS	Neurotransmission	H_3	clear	precuneus	0.764391	0.142677	0.584279	360	(0.9, 0.9, 0.1)
10	SC	Neurotransmission	$\alpha_4\beta_2$	clear	precuneus	0.763185	0.132290	0.582375	4012	(0.9, 0.9, 0.1)
					S4 (lateral temporal)					
1	**SC**	**AD-related**	***MAPT***	**mis**	**precuneus**	**0.771400**	**0.226531**	**0.413499**	**4195**	**(0.7, 1.5, 0.7)**
2	NS	Cortical expansion	scaling	syn	entorhinal	0.739296	0.240445	0.476485	126	(0.9, 3, 0.1)
3	NS	AD-related	*MAPT*	mis	precuneus	0.737158	0.207495	0.538115	29999	(0.7, 1.5, 1)
4	NS	Cortical expansion	scaling(HCP)	syn	entorhinal	0.733610	0.187773	0.467685	103	(0.7, 3, 0.7)
5	NS	Neurotransmission	VAChT	clear	entorhinal	0.716057	0.276873	0.329238	61	(0.3, 3, 1)
6	GC	Microstructure	thickness	syn	precuneus	0.715016	0.249397	0.386797	543	(0.7, 1, 0.1)
7	GC	Cortical expansion	scaling(HCP)	syn	entorhinal	0.713512	0.250491	0.318005	76	(0.3, 3, 0.7)
8	GC	AD-related	*MAPT*	spread	entorhinal	0.708057	0.199068	0.486822	314	(0.3, 3, 0.1)
9	FC	AD-related	*MAPT*	mis	precuneus	0.707129	0.236139	0.496083	218	(0.9, 3, 0.3)
10	FC	Neurotransmission	5-HT_4	mis	entorhinal	0.706228	0.218200	0.495086	252	(0.9, 3, 0.3)

Classical models originating from the entorhinal cortex (S1 and S3) or precuneus (S2 and S4) and diffusing through anatomical connections are bolded. The optimal time points (total time = 30,000) are provided, along with the selected hyperparameters: stay probability, transform rate, and velocity.

* MSE was calculated using normalized simulated tau values, scaled to match the range of observed tau.

$$EV\left(y, \hat{y}\right) = 1 - \frac{variance\{y-\hat{y}\}}{varicance\{y\}}$$

Conn = brain connectomes; R = Pearson correlation coefficient; EV = explained variance; MSE = mean squared error; syn = synthesis; mis = misfold; clear = clearance; Aβ = β amyloid; SC = structural connectivity; FC = functional connectivity; GC = gene coexpression; NS = neurotransmission markerreceptor similarity; LS = laminar similarity; MC = metabolic covariance; EP = electrophysiological; TS = temporal similarity; CBF: cerebral blood flow; CBV: cerebral blood volume; thickness: cortical thickness; scaling: allometric scalling.

Table S6. Performance of models better than null for four tau load subtypes. Related to Fig. 5.

(Attached Supplementary_Table6_Subtypes_mdoels_performance.xlsx)

The optimal time points (total time = 30,000) are provided, along with the selected hyperparameters: stay probability, transform rate, and velocity.

* MSE was calculated using normalized simulated tau values, scaled to match the range of observed tau.

$EV\left(y, \hat{y}\right) = 1 - \frac{variance\{y-\hat{y}\}}{varicance\{y\}}$

R = Pearson correlation coefficient; EV = explained variance; MSE = mean squared error; syn = synthesis; mis = misfold; clear = clearance; Aβ = β amyloid; SC = structural connectivity; FC = functional connectivity; GC = gene coexpression; NS = neurotransmission markerreceptor similarity; LS = laminar similarity; MC = metabolic covariance; EP = electrophysiological; TS = temporal similarity; CBF: cerebral blood flow; CBV: cerebral blood volume; thickness: cortical thickness; scaling: allometric scalling.

Table S7. Cluster assginment of AD-related genes identified from three GWAS studies. Related to Fig. S5 and S8.

Cluster	Gene
1	*ECHDC3, SLC2A4RG, ANK3, SIGLEC11, MAF, MS4A4A, TREM2, INPP5D, PLCG2, GRN, APH1B, PRKD3, ABCA1, FERMT2, BLNK, KLF16, ABI3, SPI1, TMEM106B, PICALM, SNX1, ADAM10, MINDY2*
2	*BIN1, ADAMTS1, APP*
3	*WNT3, EPDR1, TPCN1, SHARPIN, FOXF1, UMAD1, USP6NL, EPHA1, HS3ST5, WDR12, CD2AP*
4	*COX7C, CTSH, RBCK1, SPPL2A, IL34, TSPOAP1, BCKDK, RASGEF1C, SEC61G, CLU*
5	*IDUA, SORT1, SLC24A4, SORL1, MYO15A, ANKH, ICA1, ADAM17, DOC2A, JAZF1, EED, CTSB, KAT8, PLEKHA1, SPDYE3, TSPAN14, PTK2B, NCK2*
6	*WDR81, TNIP1, ABCA7*
7	*ACE*
Not found in AHBA	*MME, SCIMP/RABEP1, CLNK, HLA, ZCWPW1/NYAP1, SCIMP, CR1, CLNK/HS3ST1, NME8, SLC24A4/RIN3, CASS4, CELF1/SPI1, HLA-DQA1, MS4A, LILRB2, IGH gene cluster, TREML2, PRDM7, UNC5CL, RHOH*

Table S8. Full list of neurotransmission markers and derived ratios. Related to Fig. 4.

Abbr.	Full name
NMDA	**Glutamate** receptor (ionotropic; excitatory)
$mGluR_5$	Metabotropic **Glutamate** receptor type 5 (metabotropic; excitatory)
$GABA_{A/BZ}$	Ionotropic **GABA** receptor type A Benzodiazepine site (ionotropic; inhibitory)
M1	Muscarinic **Acetylcholine** receptor type 1 (metabotropic; excitatory)
$\alpha_4\beta_2$	Alpha-4 beta-2 Nicotinic **Acetylcholine** receptor (ionotropic; excitatory)
VAChT	Vesicular **Acetylcholine** transporter
$5\text{-}HT_{1A}$	**Serotonin** receptor type 1A (metabotropic; inhibitory)
$5\text{-}HT_{1B}$	**Serotonin** receptor type 1B (metabotropic; inhibitory)
$5\text{-}HT_{2A}$	**Serotonin** receptor type 2A (metabotropic; excitatory)
$5\text{-}HT_4$	**Serotonin** receptor type 4 (metabotropic; excitatory)
$5\text{-}HT_6$	**Serotonin** receptor type 6 (metabotropic; excitatory)
5-HTT	**Serotonin** transporter
NET	**Norepinephrine** transporter
D_1	**Dopamine** receptor type 1 (metabotropic; excitatory)
D_2	**Dopamine** receptor type 2 (metabotropic; inhibitory)
DAT	**Dopamine** transporter
H_3	**Histamine** receptor type 3 (metabotropic, inhibitory)
MOR	Mu-**Opioid** receptor (metabotropic, inhibitory)
CB_1	**Cannabinoid** receptor type 1 (metabotropic, -)
E:I	$(5\text{-}HT_{2A}+5\text{-}HT_4+5\text{-}HT_6+D_1+M_1+\alpha_4\beta_2+NMDA+mGluR_5)/(5\text{-}HT_{1A}+5\text{-}HT_{1B}+D_2+GABA_{A/BZ}+H_3+MOR)$
$E{:}I_{metabotropic}$	$(5\text{-}HT_{2A}+5\text{-}HT_4+5\text{-}HT_6+D_1+M_1+mGluR_5)/(5\text{-}HT_{1A}+5\text{-}HT_{1B}+D_2+H_3+MOR)$
$E{:}I_{iontropic}$	$(\alpha_4\beta_2+NMDA)/GABA_{A/BZ}$
$E{:}I_{Glu/GABA}$	$(NMDA+mGluR_5)/GABA_{A/BZ}$
$E{:}I_{Glu/GABA(ion)}$	$NMDA/GABA_{A/BZ}$
R/Re_{ACh}	$(M_1+\alpha_4\beta_2)/VAChT$
NT/NM	$(GABA_{A/BZ}+mGluR_5+NMDA)/(5\text{-}HT_{1A}+5\text{-}HT_{1B}+5\text{-}HT_{2A}+5\text{-}HT_4+5\text{-}HT_6+\alpha_4\beta_2+D_1+D_2+M_1+H_3+MOR)$
$5\text{-}HT_{1A}/5\text{-}HT_{1B}$	$5\text{-}HT_{1A}/5\text{-}HT_{1B}$
DAT/NET	DAT/NET